Phys. Status Solidi C **6**, No. 8, 1807–1810 (2009) / **DOI** 10.1002/pssc.200881463

physica status solidi c
www.pss-c.com
current topics in solid state physics

Proton backscattering by point and extended defects in ion-implanted Si

Nikolay Sobolev[*,1], **Vladimir Sakharov**[1], **Igor Serenkov**[1], **Anton Kalyadin**[1], **and Vladimir Vdovin**[2]

[1] Ioffe Physico-Technical Institute, 194021 St. Petersburg, Russia
[2] Institute for Chemical Problems of Microelectronics, 119017 Moscow, Russia

Received 17 September 2008, revised 19 December 2008, accepted 14 April 2009
Published online 17 June 2009

PACS 61.72.uj, 61.82.Fk, 68.37.Lp, 78.70.–g

[*] Corresponding author: e-mail nick@sobolev.ioffe.rssi.ru, Phone: +7 812 2973885, Fax: +7 812 2971017
Web: www.ioffe.ru

The backscattering of 230-keV protons, the depth dependences of the full width at the half minimum (FWHM) of proton angular scans and TEM were used to study the structural perfection of Si single crystals implanted with Er and Si ions at doses lower and higher than the respective amorphization thresholds. Implantation of 2-MeV Er ions at a dose of $5x10^{13}$ cm^{-2} was found to produce high concentrations of point defects without amorphization of the Si layer. After the implantation of 100-keV Si ions at a dose of $1x10^{17}$ cm^{-2} exceeding the amorphization threshold by two orders of magnitude, we observed a high density of extended defects but no amorphization. The dechanneling by point and extended defects was found to have different dependences (decreasing and increasing, respectively) of the scan FWHM on the scan depth.

1 Introduction Ion channeling is widely used to study structural perfection of crystals. In the case of ion-implanted layers, the backscattered ion energy spectra taken in a random and aligned regime can reveal structural damage and amorphous areas; one can also find the concentration profile of the implanted impurity. When implantation defects represent randomly displaced atoms, the procedure described in [1] allows one to calculate the defect profiles from the data of both energy spectra. It is found that the channeling dip FWHM in backscattering decreases with the scan depth in Si and W single crystals with a perfect lattice [2]. The dip calculations made in a continuum approximation with the account of dechanneling in Si and W perfect lattices for different penetration depths were in excellent agreement with experimental data on 0.5- and 2-MeV ^{4}He ions [2]. The measurements of 80-240 keV proton channeling in a $YBa_2Cu_3O_{7-x}$ superconductor and the Monte Carlo simulation showed that point defects of low concentration were dominant and that the dip FWHM decrease with the scan depth was due to these point defects [3]. It is hard to predict the depth dependence of the dip FWHM in crystals with other defect types. The aim of the present work was to study the depth dependence of the dip FWHM in ion-implanted Si with high concentrations of point and extended defects.

2 Experimental 2-MeV Er ions at a dose of $5x10^{13}$ cm^{-2} lower than the amorphization threshold [4] and 100-keV Si ions at a dose of $1x10^{17}$ cm^{-2} higher than the amorphization threshold [5] were implanted into (100) Si single crystals at room temperature. The structural characteristics were examined by using middle energy ion scattering (MEIS) and transmission electron microscopy (TEM). The MEIS technique uses ions with the initial energies of 50–250 keV and is a modification of the conventional Rutherford backscattering (RBS) approach dealing with 1–4 MeV ions. Since the backscattering cross section varies with the probe beam energy E as $1/E^2$, it provides a two order increase in the backscattered ion flux during the MEIS measurement as compared with RBS. Therefore, the use of MEIS is preferable in the study of thin layers with a thickness from units to several hundreds of nanometers [6]. In our experiments, the MEIS analysis involved 230-keV protons. We measured backscattered ion energy spectra for random and aligned regimes and angular scans, i.e. the dependences of the backscattered particle yield on the angle between the probing beam and the nearest low-index crystal axis, in our case the (100) direction. The measured yields were normalized to the random yield defined as the average yield in an axial scan extending to about 8° on each side of the axis. We analyzed the data on several en-

ergy windows. The depth scale was then derived in the usual way by integrating the proton stopping power in Si [7]. A semiconductor detector with the energy resolution of ~ 3.5 keV registered protons scattered to an angle of 170º. The TEM experiments were carried out on plan-view and cross-sectional samples using a JEM 200CX microscope.

3 Results and experimental Fig. 1 demonstrates the MEIS spectra measured in the random (curve 1) and aligned (curves 2 and 3) regimes from Er-implanted Si (1,2) and Si-implanted Si (1,3). The random spectra of the Er- and Si-implanted samples practically coincide, so that curve 1 represents both spectra. The ratio of the channeling to random signals in Er-implanted Si is smaller than unity in the whole range of scattered proton energies. This result indicates that the implantation of Er ions of the above energy and dose does not produce the Si layer amorphization. Previously, the absence of amorphization in Si under the same implantation conditions was observed in the study of X-ray diffraction [4]. We used the procedure of [1] and the data on both energy spectra in Fig. 1 to calculate the depth distribution of the defect concentration (Fig. 2, curve 1), assuming that the implantation defects are point defects. The defect profile was normalized to the number of Si atoms per cubic centimeter. The relative defect concentration maximum was found to be ~ 0.70 and it was located at a depth of 540 nm between the positions of the Er ion projected range (R_P ~ 555 nm) and the highest defect concentration (~ 400 nm), which were calculated using [8]. The position of the experimental profile indicates that the introduced defects were indeed point defects of high concentration.

The analysis of the MEIS spectra measured in the random (Fig. 1, curve 1) and aligned (Fig. 1, curve 3) regimes for Si-implanted Si shows that the implantation of Si ions at a dose several orders higher than the amorphization threshold (~ $1x10^{15}$ cm^{-2} [5]) produces no amorphization of the Si layer: the ratio of the channeling to random signals is smaller than unity in the whole range of scattered proton energies. This result seems quite unexpected and invites further examination. Previously, the absence of amorphization at ultrahigh doses ("effect of large doses") was observed and discussed for the case of group-III and -V ion implantation [9, 10]. Another surprising result is a strong discrepancy between the position of the maximum damage area and the Si ion projected range R_P ~ 137 nm [8]. In fact, a sharp increase in the aligned spectral intensity (curve 3) is observed at the backscattered proton energies of ~ 145 keV corresponding to the depth of 300 nm, which is essentially deeper than R_P. Like in the case of Er-implanted Si, we calculated the defect concentration profile (Fig. 2, curve 2) using the procedure of [1] and the data of both energy spectra in Fig. 1 (curves 1 and 3) on the assumption that the implantation defects were point defects. The relative defect concentration maximum is equal to ~ 0.72 and is located at the depth of 350 nm. The absence of amorphization and the much deeper position of the greatest damage area, as compared to the Si projected range, show that more complex defects were introduced and that their nature should be identified. Note also that the procedure of [1] designed for point defects only is inadequate for the calculation of concentration profiles of implantation-related defects in this case.

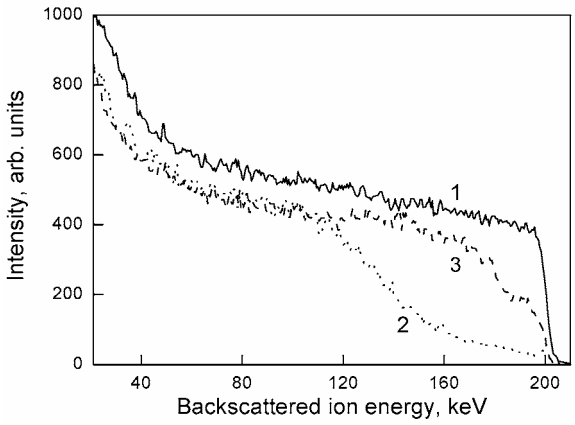

Figure 1 Spectra of proton backscattering in Si implanted with Er (1, 2) and Si (1, 3) ions, measured in (1) random and (2, 3) channeling modes.

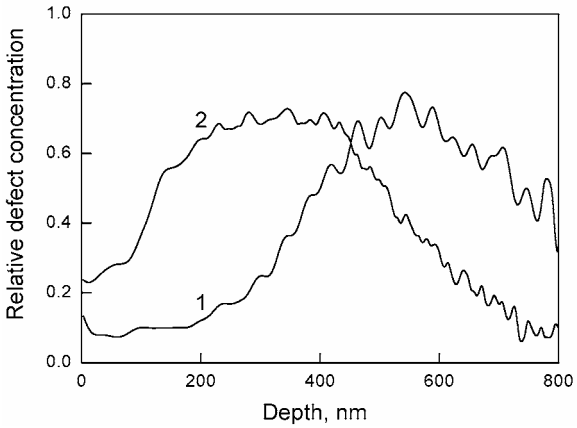

Figure 2 Normalized concentration profiles of defects in Si with implanted Er (1) and Si (2) ions.

The TEM study of the Si-implanted Si sample revealed a relatively thick (~ 480 nm) layer containing extended structural defects of high density (> 10^{10} cm^{-2}). The transmission electron diffraction pattern of this layer contained distinct diffraction spots corresponding to single crystal Si. No sings of amorphous or secondary phases were detected. The examination of the thinnest parts of the foil revealed single elements of electron microscopic contrast indicating the presence of dislocations. Additionally, we observed individual two-dimensional defects located on the inclined {111} atomic planes at the layer top, which are likely to be stacking faults. This defect structure fundamentally differs from that usually formed during recrystallization of preamorphized silicon layers in solid phase epitaxy (SPE). An obligatory element of the SPE layers is a narrow band of

end-of-range (EOR) defects inside the silicon wafer in the amorphous-crystal transition zone. Another characteristic feature of the SPE layers is a high density of threading hairpin dislocations [11].

The experimental dips for proton backscattering by an Er-implanted Si crystal along the (100) axis at various depths are shown in Fig. 3. The scans were measured in the layers of 100 nm thickness. One can see that the minimum yield increases and the dip FWHM decreases with the scan depth. These results were predictable since this effect is associated with proton dechanneling by implantation-related point defects. The dip FWHM values are equal to 1.5 and 1.4º for the depths of 100 and 450 nm corresponding to the areas with the minimum and maximum concentrations of implantation-related point defects, respectively (Fig. 2, curve 1). This observation is similar to that for single crystals with a perfect lattice [2] and a low concentration of point defects [3]. Thus, the measured dip FWHM decreases with depth in single crystals containing a high concentration of introduced point defects.

The experimental dips from the proton backscattering by the Si-implanted Si crystal along the (100) axis at various depths are shown in Fig. 4. The thickness of the layers, in which the backscattered protons were registered during the scan measurements, was ~ 70 nm. The observable increase in the minimum yield with the scan depth is due to the proton dechanneling by implantation-related extended defects. The dip FWHM values are 2.1, 2.8 and 4.4º at the depths of 65, 150 and 345 nm, respectively. An increase in

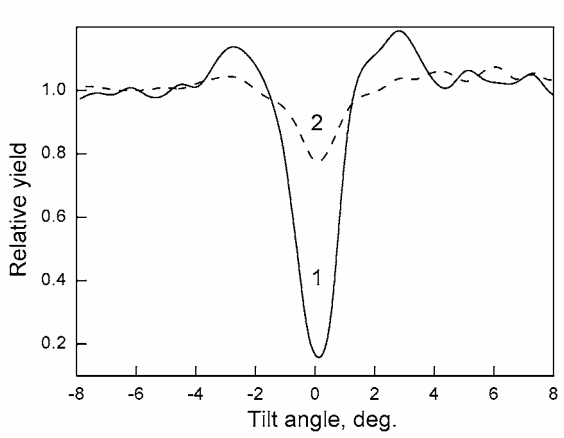

Figure 3 Normalized yield of backscattered protons at the depths of 100 (1) and 450 (2) nm in Er-implanted Si.

the dip FWHM with increasing depth was observed for the first time and was attributed to proton dechanneling by the introduced extended defects. It may be pointed out that the measurement of angular scans for 2-MeV He ion dechanneling showed practically no difference between the FWHM values for a virgin Al crystal and Al crystals implanted with Al or Zn ions and containing dislocations with a density of ~ 10^{11} cm^{-2} [12]. Apparently, this result was due to the fact that the thickness of the layer, in which the backscattered ion scans were measured (200 nm), was larger than that of the defect-containing area (40 nm). Therefore, the opposite dip FWHM dependences on the scan depth in crystals containing extended defects (a rising curve) and crystals with a perfect lattice or point defects in different concentrations (a falling curve) can be used for pre-identification of defects.

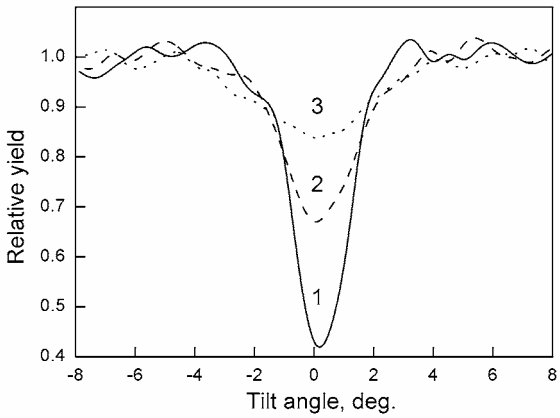

Figure 4 Normalized yield of backscattered protons at the depths of 65 (1), 150 (2) and 345 (3) nm in Si-implanted Si.

4 Conclusions Thus, the results presented here show that room temperature implantation of 2-MeV Er ions at a dose of 5x10^{13} cm^{-2} and 100-keV Si ions at a dose of 1x10^{17} cm^{-2} does not lead to Si amorphization but introduces point defects of high concentration or extended defects of high density, respectively. Further research effort is necessary to understand the effects of zero amorphization at an ion dose exceeding the amorphization threshold by two orders and extended defect introduction during the implantation. The observed result is reliable since it was obtained by two independent techniques. The ascertained possibility to produce a relatively thick layer with extended defects of high concentration is of practical importance for fabrication of Si-based light-emitting diodes with dislocation-related luminescence [5]. We have found that the dip FWHM increase with the scan depth occurs in crystals with a high density of extended defects in contrast to the dip FWHM decrease observed in crystals containing a high concentration of point defects. The relationship between the dip FWHM and the layer depth gives a chance to identify dominant structural defects, point or extended ones.

Acknowledgements This work was partly supported by the Russian Foundation for Basic Research (Grants 07-02-01462, 08-02-000893) and by the Joint Research Center "Material Science and Characterization in Advanced Technologies".

References

[1] L. C. Feldman, J. W. Mayer, and S. T. Picraux, Material Analysis by Ion Channeling (Academic Press, N.Y., 1982), Chap. 5.

[2] E. F. Kennedy, B. Bech Nielsen, and J. U. Andersen, NIMS B **67**, 236 (1992).

[3] V. V. Afrosimov, G. O. Dzyuba, R. N. Il`in, M. N. Panov, V. I. Sakharov, I. T. Serenkov, and E. A. Ganza, Tech. Phys. **41**(12), 1240 (1996).
[4] R. N. Kyutt and N. A. Sobolev, Phys. Solid State **39**, 759 (1997).
[5] N. A. Sobolev, A. M. Emel`yanov, V. I. Sakharov, I. T. Serenkov, and D. I. Tetel`baum, Semiconductors **41**, 537 (2007).
[6] V. V. Afrosimov, R. N. Il`in, V. I. Sakharov, and I. T. Serenkov, Semiconductors **41**, 497 (2007).
[7] J. F. Ziegler, The Stopping and Ranges of Ions in Matter, Vol. 4 (Pergamon, New York, 1977).
[8] http://www.srim.org
[9] N. N. Gerasimenko, A. V. Dvurechenski, S. I. Romanov, and L. S. Smirnov, Sov. Phys. Semicond. **7**, 1461 (1973).
[10] D. I. Tetel'baum and A. I. Gerasimov, Semiconductors **38**, 1260 (2004).
[11] C. Carter, W. Maszara, D. K. Sadana, G. A. Rozgonyi, J. Liu, and J. Wortman, Appl. Phys. Lett. **44**, 459 (1984).
[12] S. T. Picraux, E. Rimini, G. Foti, and S. U. Campisano, Phys. Rev. B **18**, 2078 (1978).

